

# MODELING THE MULTI-BAND AFTERGLOW OF GRB 060614: FURTHER EVIDENCE FOR A DOUBLE POWER-LAW HARD ELECTRON ENERGY SPECTRUM

Q. ZHANG,<sup>1</sup> S. L. XIONG,<sup>1</sup> AND L. M. SONG<sup>1</sup>

<sup>1</sup>*Key Laboratory of Particle Astrophysics, Institute of High Energy Physics, Chinese Academy of Sciences, Beijing 100049, China*

(Received; Revised; Accepted)

Submitted to ApJ

## ABSTRACT

Electrons accelerated in relativistic collisionless shocks are usually assumed to follow a power-law energy distribution with an index of  $p$ . Observationally, although most gamma-ray bursts (GRBs) have afterglows that are consistent with  $p > 2$ , there are still a few GRBs suggestive of a hard ( $p < 2$ ) electron energy spectrum. Our previous work showed that GRB 091127 gave tentative evidence for a double power-law hard electron energy (DPLH) spectrum with  $1 < p_1 < 2$ ,  $p_2 > 2$  and an “injection break” assumed as  $\gamma_b \propto \gamma^q$  in the relativistic regime, where  $\gamma$  is the bulk Lorentz factor of the jet. In this paper, we show that GRB 060614 provides further evidence for such a DPLH spectrum. Similar to GRB 091127, the afterglow of this burst shows an early flat spectrum in the optical/ultraviolet (UV) band and a spectral break passing through this band between  $\sim 10$  and  $\sim 30$  ks. Differently, the X-ray/UV light curves exhibit an initial plateau lasting about 30 ks. We thus extend the theory of Resmi & Bhattacharya (2008) by taking into account an additional energy injection process and model the multi-band afterglow of GRB 060614. Along with the results of GRB 091127, our work suggests a possibly universal DPLH spectrum with  $p_2 - p_1 \sim 1$  and  $q \sim 0.5$ . However, more such afterglow observations are needed to test this conjecture.

*Keywords:* acceleration of particles – gamma-ray burst: individual (GRB 060614) – ISM: jets and outflows – radiation mechanisms: non-thermal

## 1. INTRODUCTION

Gamma-Ray bursts (GRBs) are the most energetic stellar explosions in the universe. They produce a short prompt  $\gamma$ -ray emission followed by a long-lived afterglow phase. The afterglows of GRBs are believed to originate from the synchrotron emission of shock-accelerated electrons produced by the interaction between the outflow and the external medium (Rees & Mészáros 1992; Mészáros & Rees 1993, 1997; Sari et al. 1998; Chevalier & Li 2000). Particle acceleration is usually attributed to the *Fermi* process (Fermi 1954), which results in a power-law (PL) energy distribution  $N(E)dE \propto E^{-p}dE$ , with a cutoff at high energies. Some analytical and numerical studies indicate a nearly universal spectral index of  $p \sim 2.2 - 2.4$  (e.g., Bednarz & Ostrowski 1998; Kirk et al. 2000; Achterberg et al. 2001; Lemoine & Pelletier 2003; Spitkovsky 2008), though other studies suggest that there is a large range of possible values for  $p$  of  $1.5 - 4$  (Baring 2004). The values of  $p$  derived from the spectral analysis of the multi-band afterglow (e.g. Chevalier & Li 2000; Panaitescu & Kumar 2002; Starling et al. 2008; Curran et al. 2009; Fong et al. 2015; Li et al. 2015; Wang et al. 2015) or the X-ray data alone (e.g., Shen et al. 2006; Curran et al. 2010) show a rather wide distribution, but most of them are consistent with  $p > 2$ . Only a few GRBs, e.g., GRB 060908 (Covino et al. 2010), GRB 091127 (Filgas et al. 2011; Troja et al. 2012) and GRB 140515A (Melandri et al. 2015), show very flat spectra in the optical band and require a hard ( $p < 2$ ) electron energy spectrum.

To explain those afterglows that cannot be well modeled with a standard ( $p \gtrsim 2$ ) electron energy spectrum, two types of electron energy distributions were proposed in literature: (1) a single PL electron energy distribution ( $1 < p < 2$ ) with an exponential cutoff at a maximum electron Lorentz factor  $\gamma_M$  (Bhattacharya 2001; Dai & Cheng 2001); (2) a double PL electron energy distribution ( $1 < p_1 < 2$  and  $p_2 > 2$ ) with an “injection break”  $\gamma_b$  (Panaitescu & Kumar 2001; Bhattacharya & Resmi 2004; Resmi & Bhattacharya 2008; Wang et al. 2012). A direct method to distinguish the two models is to see the passage of the injection break frequency  $\nu_b$  (i.e., the synchrotron frequency corresponding to  $\gamma_b$ ) through a certain band, e.g, from the optical to the near-infrared (NIR) bands. Our previous work (Zhang et al. 2015, Paper I hereafter) showed that GRB 091127 was such a case and gave tentative evidence for the double PL hard electron spectrum model (the so-called “DPLH model” in Paper I). For this burst, the electron energy spectrum exhibits two features: (i)  $p_2 - p_1 \approx 1$ ; (ii)  $\gamma_b \propto \gamma^q$  with  $q \sim 0.6$ , here  $\gamma$  is the bulk

Lorentz factor of the jet. Do they imply a universal law of the DPLH spectrum? With only one case so far, we cannot give the answer.

In this paper, we show that the multi-band afterglow of GRB 060614 provides further evidence for a DPLH spectrum. GRB 060614 is a remarkable burst with puzzling properties both in prompt and afterglow emissions (Mangano et al. 2007, M07 hereafter). It is a long-duration nearby event, while the lack of a supernova association and its null temporal lag put it into the short-GRB subclass (Della Valle et al. 2006; Fynbo et al. 2006; Gal-Yam et al. 2006; Gehrels et al. 2006; Zhang et al. 2007). After the initial fast decay, the X-ray afterglow shows a plateau before  $T_{X,b1} \sim 36$  ks, followed by a normal decay phase, then it further steepens at  $T_{X,b2} \sim 104$  ks which was identified as a jet break (M07). The two achromatic breaks are observed simultaneously in the optical and ultraviolet (UV) bands. The above light curve (LC) behaviors are not uncommon in the *Swift* era (e.g., Nousek et al. 2006; Zhang et al. 2006; Evans et al. 2009; Zaninoni et al. 2013; Li et al. 2015). What is puzzling, however, is that the optical/UV LCs exhibit strong spectral evolution before  $T_{X,b1}$  and the decay slopes<sup>1</sup> range from  $\sim (-0.38)$  to  $\sim 0.27$ , depending on wavelength (M07). Detailed spectral analysis of M07 showed that the observed spectral evolution is caused by the passage of a break frequency through the optical/UV band. During this phase, the optical data show a rather flat spectrum with  $\beta_{\text{opt}} \sim 0.3$  and the difference of spectral indices between the optical and X-ray bands is  $\Delta\beta = \beta_X - \beta_{\text{opt}} \sim 0.5$  (M07). So the key to the problem is to find which kind of break frequency can produce the observed behavior.

Neither the minimum synchrotron frequency  $\nu_m$  nor the cooling frequency  $\nu_c$  can accommodate the above observations. The reasons are as follows: (i) Although the passage of  $\nu_m$  can produce a spectral evolution and slow-rising optical LCs (M07), this requires  $\nu_{\text{opt}} < \nu_m$ . The model predicted spectral index in this regime is  $\beta_{\text{opt}} = -1/3$  which is inconsistent with the observed value ( $\sim 0.3$ ); (ii) If the observed break frequency is  $\nu_c$ , it suggests a hard electron energy spectrum with  $p = 2\beta_{\text{opt}} + 1 \sim 1.6$ . However, the single PL hard electron spectrum model of Dai & Cheng (2001) predicts the post-jet-break decay slope should be  $\sim 1.9$  which is substantially lower than the observed value ( $\sim 2.4$ ; M07).

<sup>1</sup> The convention  $F_\nu \propto \nu^{-\beta} t^{-\alpha}$  is adopted throughout the paper, where  $\beta$  is the spectral index and  $\alpha$  is the temporal decay index. With this convention, hereafter the term “decay slope(s)” denotes the value(s) of  $\alpha$ .

Similar to the afterglow modeling of GRB 091127 (Paper I), in this work we explain the multi-band afterglow of GRB 060614 with the DPLH model. To produce the plateau-like feature in the X-ray and UV LCs, we extend the original DPLH model by taking into account an additional energy injection process (Sari & Mészáros 2000; Zhang & Mészáros 2001). Besides modeling the afterglow data, our most concern is to find out whether the two cases have a similar DPLH spectrum, especially on the evolution of the injection break  $\gamma_b$ . Either a positive or a negative result would be invaluable for our knowledge of the particle acceleration process in relativistic collisionless shocks.

Our paper is organized as follows. In Section 2, we summarize the observational results of GRB 060614. The DPLH model with a continuous energy injection is described in Section 3. In Section 4, we constrain the model parameters and then compare our model with the multi-band afterglow data. Finally, we present our conclusion and make some discussions in Section 5. Throughout the paper, we use the standard notation  $Q_x = Q/10^x$  with  $Q$  being a generic quantity in cgs units, and a concordance cosmology with parameters  $H_0 = 70 \text{ km s}^{-1} \text{ Mpc}^{-1}$ ,  $\Omega_M = 0.27$ , and  $\Omega_\Lambda = 0.73$  is adopted (Jarosik et al. 2011). All the quoted errors are given at a  $1\sigma$  confidence level (CL) unless stated otherwise.

## 2. OBSERVATIONAL RESULTS

GRB 060614 triggered the *Swift* Burst Alert Telescope (BAT; Barthelmy et al. 2005) on 2006 June 14 at  $T_0 = 12:43:48 \text{ UT}$  (Parsons et al. 2006) and was also detected by *Konus-Wind* (Golenetskii et al. 2006). The LC shows an initial hard, bright peak lasting  $\sim 5 \text{ s}$  followed by a long, somewhat softer extended emission, with a total duration of  $T_{90}(15 - 350 \text{ keV}) = 102 \pm 3 \text{ s}$  (Barthelmy et al. 2006). The spectrum of the initial pulse can be fitted in the 20 keV–2 MeV energy range by a PL with an exponential cutoff model, with the peak energy  $E_{\text{pk}} \sim 302 \text{ keV}$ , while the spectrum of the remaining part of the burst can be described by a simple PL with photon index  $2.13 \pm 0.03$  (Golenetskii et al. 2006). The total fluence in the 20 keV–2 MeV energy range is  $\sim 4.1 \times 10^{-5} \text{ erg cm}^{-2}$ , of which the initial intense pulse contributes a fraction of  $\sim 20\%$  (Golenetskii et al. 2006). With a redshift of  $z = 0.125$  (Fugazza et al. 2006; Price et al. 2006), the isotropic equivalent energy was estimated as  $E_{\gamma, \text{iso}} = (2.5 \pm 0.4) \times 10^{51} \text{ erg}$  in the  $1 - 10^4 \text{ keV}$  rest-frame energy band (M07). In addition, GRB 060614 has null spectral lags, being consistent with typical short GRBs (Gehrels et al. 2006).

The X-ray Telescope (XRT; Burrows et al. 2005) began observing the field 91 s after the BAT trigger (Parsons et al. 2006). The X-ray afterglow of GRB 060614 exhibits a canonical LC which has been commonly observed in the *Swift* era (e.g., Nousek et al. 2006; Zhang et al. 2006; Evans et al. 2009). It begins with an initial fast exponential decay, followed by a plateau with slope  $\alpha_{X,1} = 0.11 \pm 0.03$ ; at  $T_{X,b1} = 36.6 \pm 1.5 \text{ ks}$ , it steepens to a standard afterglow evolution with slope  $\alpha_{X,2} = 1.03 \pm 0.01$ ; later on, the LC shows a further steepening to a slope  $\alpha_{X,3} = 2.13 \pm 0.04$  at  $T_{X,b2} = 104 \pm 13 \text{ ks}$  (M07). The X-ray data observed in the photon counting (PC) mode show no significant spectral evolution, with the spectral index  $\beta_X \sim 0.8$  (M07).

The *Swift* Ultra-Violet/Optical Telescope (UVOT; Roming et al. 2005) commenced observations 101 s after the BAT trigger (Holland 2006). Besides, the R-band afterglow was detected by several ground telescopes (e.g., Della Valle et al. 2006; French et al. 2006; Fynbo et al. 2006; Gal-Yam et al. 2006). M07 presented detailed spectral and temporal analysis of the optical/UV afterglow, below we summarize their main results. The optical/UV LCs show achromatic breaks with the X-ray afterglow, i.e.,  $t_{\text{UV0,b1}} = 29.7 \pm 2.7 \text{ ks}$  and  $t_{\text{UV0,b2}} = 117.2 \pm 2.7 \text{ ks}$ . The decay slopes after the two breaks are  $\alpha_{\text{UV0,2}} = 1.11 \pm 0.03$  and  $\alpha_{\text{UV0,3}} = 2.44 \pm 0.05$ , respectively. On the whole, the X-ray/UV/optical LCs have marginally consistent evolutions after  $\sim 30 \text{ ks}$ . What is puzzling is that the initial slope  $\alpha_{\text{UV0,1}}$  is dependent on wavelength: the UV LCs show nearly flat evolutions while the optical LCs rise slowly with slopes from  $\sim (-0.38)$  to  $\sim (-0.17)$ . The spectral energy distributions (SEDs) of the afterglow from optical to X-rays show a spectral break passing through the optical/UV band between  $\sim 10$  and  $\sim 30 \text{ ks}$ . The break frequency at 10 ks is around  $1.0 \times 10^{15} \text{ Hz}$  (see Figure 7 of M07). At this time, the optical/UV and X-ray afterglows have spectral indices  $\beta_{\text{UV0}} = 0.30 \pm 0.09$  and  $\beta_X = 0.84 \pm 0.04$ , respectively. At later times ( $t \gtrsim 30 \text{ ks}$ ), the spectral index in the optical/UV band changes to be consistent with that of X-rays. Fits of the broad-band SEDs imply a weak host extinction  $A_{V,h} = 0.05 \pm 0.01$  (M07).

In addition, deep optical/NIR follow-ups of GRB 060614 show no evidence for an associated supernova down to very strict limits; the GRB host is a very faint star-forming galaxy with a specific star formation rate lower than most long GRB hosts; the GRB counterpart resides in the outskirts of the host (Della Valle et al. 2006; Fynbo et al. 2006; Gal-Yam et al. 2006). The recent discovery of a distinct NIR excess at about 13.6 days after

the burst suggests a possible kilonova (or macronova) origin (Jin et al. 2015; Yang et al. 2015). Together with the vanishing time lags of the prompt emission, all these point towards a different origin from typical long GRBs; it is likely to be of a subclass of merger-type short GRBs (Gehrels et al. 2006; Zhang et al. 2007).

### 3. MODEL

Several clues should be considered before establishing the afterglow model for GRB 060614: (i) The two achromatic breaks ( $t_{b,1} \equiv t_{\text{UVO},b1} \approx t_{X,b1}$  and  $t_{b,2} \equiv t_{\text{UVO},b2} \approx t_{X,b2}$ ) shown in the multi-band LCs require a hydrodynamical origin. This canonical afterglow behavior was well described in Zhang et al. (2006). The first break is possibly an “energy-injection break”, implying the end of a continuous energy injection into the forward shock (Sari & Mészáros 2000; Zhang & Mészáros 2001), while the second break is most likely the so-called “jet break” (Rhoads 1999; Sari et al. 1999); (ii) The early flat spectrum ( $\beta_{\text{UVO}} \sim 0.3$ ) in the optical/UV band definitely requires a hard electron energy spectrum; (iii) As stated in Section 1, the single PL hard electron spectrum model with  $\nu_{\text{UVO}} < \nu_c < \nu_X$  can be excluded, so the DPLH model is a natural choice. In this section, we extend the original DPLH model of Resmi & Bhattacharya (2008) by taking into account an additional energy injection process.

The DPLH spectrum with indices  $1 < p_1 < 2$  and  $p_2 > 2$  is represented as (Resmi & Bhattacharya 2008)

$$N(\gamma_e) = C_e \begin{cases} \left(\frac{\gamma_e}{\gamma_b}\right)^{-p_1}, & \gamma_m \leq \gamma_e < \gamma_b, \\ \left(\frac{\gamma_e}{\gamma_b}\right)^{-p_2}, & \gamma_e \geq \gamma_b, \end{cases} \quad (1)$$

where  $C_e$  is the normalization constant,  $\gamma_m$  is minimum electron Lorentz factors, and  $\gamma_b$  is the injection break. The physical origin of  $\gamma_b$  is not clear, Resmi & Bhattacharya (2008) assumed that it is a function of  $\beta\gamma$  to accommodate the non-relativistic regime of expansion, i.e.,

$$\gamma_b = \xi (\beta\gamma)^q, \quad (2)$$

where  $\xi$  is a constant of proportionality,  $\beta = \sqrt{1 - \gamma^{-2}}$  is the dimensionless bulk velocity, and  $q$  is assumed to be a constant for simplicity.

For a relativistic shock propagating through a cold medium with particle density  $n$ , the post-shock particle density and energy density are  $4\gamma n$  and  $4\gamma(\gamma - 1)nm_p c^2$ , respectively (Sari et al. 1998), from which one derives the minimum Lorentz factor (Resmi & Bhattacharya

2008)

$$\gamma_m = \left(f_p \frac{m_p}{m_e} \frac{\epsilon_e}{\xi^{2-p_1}}\right)^{\frac{1}{p_1-1}} \beta^{-\frac{q(2-p_1)}{p_1-1}} (\gamma - 1)^{\frac{1}{p_1-1}} \gamma^{-\frac{q(2-p_1)}{p_1-1}}, \quad (3)$$

where  $m_p$  and  $m_e$  are the proton and electron rest mass, respectively;  $\epsilon_e$  is the fraction of shock energy carried by electrons, and  $f_p = [(2 - p_1)(p_2 - 2)] / [(p_1 - 1)(p_2 - p_1)]$ .

We calculate the break frequencies of synchrotron spectra  $\nu_m$ ,  $\nu_b$ ,  $\nu_c$  and the peak flux  $F_{\nu, \text{max}}$  according to the formula given by Wijers & Galama (1999):

$$\nu_m = \frac{x_p}{1+z} \frac{q_e B'}{\pi m_e c} \gamma \gamma_m^2, \quad (4)$$

$$\nu_{b,c} = \frac{0.286}{1+z} \frac{q_e B'}{\pi m_e c} \gamma \gamma_{b,c}^2, \quad (5)$$

$$F_{\nu, \text{max}} = \frac{\sqrt{3} \phi_p N_e q_e^3 (1+z)}{4\pi d_L^2 m_e c^2} B' \gamma, \quad (6)$$

where  $N_e$  is the total number of swept-up electrons,  $q_e$  is the electron charge,  $B' = (32\pi n m_p c^2 \epsilon_B)^{1/2} \gamma$  is the post-shock magnetic field density,  $\epsilon_B$  is the fraction of shock energy carried by magnetic fields,  $d_L$  is the luminosity distance corresponding to the redshift  $z$ ,  $\gamma_c = 6\pi m_e c / (\sigma_T \gamma B'^2 t)$  is the cooling Lorentz factor of electrons.  $x_p$  and  $\phi_p$  represent the dimensionless peak frequency and the peak flux, respectively. Their dependence on  $p$  can be obtained from Wijers & Galama (1999).

The calculation of break frequencies and peak flux given above depends on the hydrodynamic evolution of the shock. For the case of GRB 060614, the hydrodynamics should undergo three phases: a process of continuous energy injection, an adiabatic evolution and a post-jet-break evolution. Below we give a simple description of these physical processes.

(I) *decelerating blastwave with and without energy injection*

The injected energy can be provided by a long-lived central engine (Dai & Lu 1998; Zhang & Mészáros 2001) or by slower material with significant energy which gradually piles up onto the decelerating ejecta and “refreshes” it (Resmi & Mészáros 1998; Sari & Mészáros 2000). Here we do not consider a specific energy injection mechanism and generally assume that the isotropic equivalent blastwave energy  $E$  evolves as

$$E(t) = \begin{cases} E_f \left(\frac{t}{t_f}\right)^{1-e}, & t_i \leq t < t_f, \\ E_f, & t \geq t_f, \end{cases} \quad (7)$$

where  $t_i$  is the time when the assumed PL energy injection ( $E \propto t^{1-e}$ ) begins,  $t_f$  is the end time of the energy



injection,  $E_f$  is the final blastwave energy, and  $e < 1$  is required for an effective energy injection.

Considering the short-GRB-like properties of GRB 060614, a homogeneous interstellar medium (ISM) circumburst environment is reasonably assumed. In fact, using the LC decay slopes given in Table 2 of Resmi & Bhattacharya (2008), one can easily exclude a wind-like medium for this burst. For the self-similar evolution of an adiabatic blastwave in the ISM case (Blandford & McKee 1976; Sari et al. 1998), the expressions of  $\nu_m$ ,  $\nu_c$ ,  $\nu_b$  and  $F_{\nu, \max}$  have been derived in Paper I and are listed below<sup>2</sup>:

$$\nu_m = 8.2 \times 10^6 (1833 f_p)^{\frac{2}{p_1-1}} (37.2)^{\frac{1-q(2-p_1)}{p_1-1}} \frac{x_{p_1}}{1+z} \xi^{-\frac{2(2-p_1)}{p_1-1}} \epsilon_e^{\frac{2}{p_1-1}} \epsilon_{B,-2}^{1/2} E_{52}^{\frac{p_1-q(2-p_1)}{4(p_1-1)}} n_0^{\frac{p_1-2+q(2-p_1)}{4}} \left( \frac{t_d}{1+z} \right)^{\frac{-3[p_1-q(2-p_1)]}{4(p_1-1)}} \text{ Hz}, \quad (8)$$

$$\nu_c = 1.5 \times 10^{15} \epsilon_{B,-2}^{-3/2} E_{52}^{-1/2} n_0^{-1} [t_d(1+z)]^{-1/2} \text{ Hz}, \quad (9)$$

$$\nu_b = 3.8 \times 10^5 \frac{(6.1)^{1+2q}}{1+z} \xi^2 \epsilon_{B,-2}^{1/2} E_{52}^{\frac{1+q}{4}} n_0^{\frac{1-q}{4}} \left( \frac{t_d}{1+z} \right)^{\frac{-3(1+q)}{4}} \text{ Hz}, \quad (10)$$

$$F_{\nu, \max} = 6.8 \times 10^3 \phi_{p_1} \epsilon_{B,-2}^{1/2} E_{52} n_0^{1/2} d_{L,28}^{-2} (1+z) \mu\text{Jy} \quad (11)$$

where  $t_d$  is the time in days. When the energy injection is taken into account, the blastwave energy  $E$  in the above equations should be replaced with Equation (7).

The evolution of the synchrotron flux density at a given frequency ( $F_\nu$ ) relies on the order of the three break frequencies and the regime in which  $\nu$  resides. Here and below we give only some scaling laws<sup>3</sup> for  $F_\nu$  and  $\nu_b$  that will be used in Section 4. For  $\nu_m < \nu < \nu_b < \nu_c$ ,

$$F_\nu = F_{\nu, \max} \left( \frac{\nu}{\nu_m} \right)^{-\frac{p_1-1}{2}} \propto t^{\left[ (1-e) - \frac{(2+e)(p_1+p_1q-2q)}{8} \right]}. \quad (12)$$

For  $\nu_m < \nu_b < \nu < \nu_c$ ,

$$F_\nu = F_{\nu, \max} \left( \frac{\nu_b}{\nu_m} \right)^{-\frac{p_1-1}{2}} \left( \frac{\nu}{\nu_b} \right)^{-\frac{p_2-1}{2}}$$

<sup>2</sup> For simplification, the effect of sideways expansion on the hydrodynamic evolution was neglected in these derivations. It can be seen as a reasonable approximation since the jet is highly relativistic.

<sup>3</sup> We refer the reader to Resmi & Bhattacharya (2008) for a complete reference of the scaling relationships for the spectral breaks and  $F_\nu$  in various spectral regimes (but without an energy injection).

$$\propto t^{\left[ (1-e) - \frac{(2+e)(p_2+p_2q-2q)}{8} \right]}. \quad (13)$$

According to Equation (10), the injection break frequency  $\nu_b$  scales as

$$\nu_b \propto t^{-\frac{(2+e)(1+q)}{4}}. \quad (14)$$

After the end of the energy injection ( $t \geq t_f$ ), the blastwave enters an adiabatic evolution phase and the corresponding scaling relationships can be easily obtained by setting  $e = 1$  in Equations (12)–(14).

## (II) post-jet-break evolution

For a simplified conical jet with a half-opening angle  $\theta_j$ , as it decelerates, the radiation beaming angle ( $1/\gamma$ ) would eventually exceed the jet half-opening angle, i.e.,  $1/\gamma > \theta_j$ . At this time, a jet break may occur in the afterglow LC. Two effects could result in a jet break: the first is the pure jet-edge effect which steepens the LC by  $t^{-3/4}$  for an ISM medium (Mészáros & Rees 1999); the second effect is caused by sideways expansion, which has important effects on the hydrodynamics when  $1/\gamma \gtrsim \theta_j$  is satisfied and the post-jet-break flux decays as  $t^{-p}$  for a normal electron energy spectrum with index  $p > 2$  (Rhoads 1999; Sari et al. 1999).

For GRB 060614, the jet break should be a result of significant sideways expansion rather than the jet-edge effect. The reasons are as follows: (i) The post-jet-break decay (in the optical/UV band) caused by the edge effect would have a slope  $\sim 1.1 + 0.75 = 1.85$ , which is substantially lower than the observed value ( $\sim 2.44$ ); (ii) Using the expression (their Equation (11)) given by Wang et al. (2012) who considered the effect of sideways expansion in a similar DPLH model and the obtained parameter values ( $p_2$  and  $q$ ) in our Section 4, we estimate the post-jet-break slope to be  $\sim 2.48$  which is excellently consistent with the observed.

Based on the work of Wang et al. (2012), we give the scaling law for  $F_\nu$  in the post-jet-break phase straightforwardly. For  $\nu_m < \nu_b < \nu < \nu_c$ ,

$$F_\nu \propto t^{-\frac{q(p_2-2)+(p_2+2)}{2}}, \quad t > t_j, \quad (15)$$

where  $t_j$  is the jet-break time.

## 4. PARAMETER CONSTRAINT AND AFTERGLOW MODELING

Before constraining the free parameters ( $p_1$ ,  $p_2$ ,  $q$ ,  $e$ ,  $\epsilon_e$ ,  $\epsilon_B$ ,  $\xi$ ,  $E_f$  and  $n$ ), we first summarize the relevant observational results of GRB 060614: (i)  $\beta_{\text{UVO}}(10 \text{ ks}) = 0.30 \pm 0.09$ ,  $\beta_X = 0.84 \pm 0.04$ ; (ii)  $\alpha_{X,1} = 0.11 \pm 0.03$ ;  $\alpha_{\text{UVO},2} = 1.11 \pm 0.03 \approx \alpha_{X,2}$ ; (iii)  $t_{b,1} = 29.7 \pm 2.7 \text{ ks}$ ,

$t_{b,2} = 117.2 \pm 2.7$  ks; (iv)  $\tilde{\nu}_b(10 \text{ ks}) \approx 1.0 \times 10^{15} \text{ Hz}^4$ ; (v)  $\tilde{\nu}_b(30 \text{ ks}) \lesssim \nu_R$ , since the SED shows that the break frequency has just crossed the R-band at about 30 ks; (vi) the initial decay slope of the R-band LC  $\alpha_{R,1} = -0.38 \pm 0.14$ ; (vii)  $\alpha_{\text{UVO},3} = 2.44 \pm 0.05 \approx \alpha_{X,3}$ . In this section we use conditions (i)–(iv) to constrain the model parameters, and use (v)–(vii) to for consistency checks.

Using condition (i), we get  $p_1 = 2\beta_{\text{UVO}}(10 \text{ ks}) + 1 = 1.60 \pm 0.18$  and  $p_2 = 2\beta_X + 1 = 2.68 \pm 0.08$ . The values of  $q$  and  $e$  can be obtained from condition (ii) and Equation (13), i.e.,

$$\frac{(2+e)(p_2 + p_2q - 2q)}{8} - (1-e) = 0.11 \pm 0.03, \quad (16)$$

$$\frac{3(p_2 + p_2q - 2q)}{8} = 1.11 \pm 0.03. \quad (17)$$

Solving these equations gives  $q = 0.41 \pm 0.20$  and  $e = 0.27 \pm 0.04$ . With these values, we test our model predictions with conditions (v)–(vii). First, Equation (14) gives  $\nu_b \propto t^{-0.80 \pm 0.12}$  during the energy injection phase, then, with condition (iv) we have  $\nu_b(30 \text{ ks}) \approx 4.2 \times 10^{14} \text{ Hz}$ , which is excellently consistent with condition (v). Second, based on Equation (12), the predicted initial R-band decay slope is  $-0.32 \pm 0.09$  that is consistent with the observational results (condition (vi)) within  $1 \sigma$  errors. Finally, we estimate the post-jet-break decay slope from Equation (15) and the obtained value is  $2.48 \pm 0.09$ , which is in perfect accord with that of the optical/UV afterglow, and marginally consistent with that of the X-ray afterglow. These exciting results encourage us to have a further check of our model by modeling the afterglow LCs. In the following calculations, we adopt  $p_1 = 1.6$ ,  $p_2 = 2.68$ ,  $q = 0.41$  and  $e = 0.27$ .

In the normal decay phase ( $t_{b,1} < t < t_{b,2}$ ), we have  $\nu_m < \nu_b < \nu_{\text{UVO}} < \nu_X < \nu_c$ . Following Equations (8)–(11) and (13), one derives<sup>5</sup>

$$\nu_m = 1.1 \times 10^{10} \xi_4^{-1.33} \epsilon_{e,-1}^{3.33} E_{f,52}^{0.6} n_0^{-0.06} t_d^{-1.8} \text{ Hz} \quad (18)$$

$$\nu_b = 1.0 \times 10^{15} \xi_4^2 \epsilon_{B,-2}^{1/2} E_{f,52}^{0.35} n_0^{0.15} t_d^{-1.06} \text{ Hz}, \quad (19)$$

$$\nu_c = 1.4 \times 10^{15} \epsilon_{B,-2}^{-3/2} E_{f,52}^{-1/2} n_0^{-1} t_d^{-1/2} \text{ Hz}, \quad (20)$$

$$F_{\nu_R} = 7.5 \times 10^3 \xi_4^{0.68} \epsilon_{e,-1}^{0.92} E_{f,52}^{1.37} n_0^{0.56} t_d^{-1.11} \mu\text{Jy}. \quad (21)$$

<sup>4</sup> Here and below we use  $\tilde{\nu}_b$  to denote the observed break frequency in the SEDs, in order to distinguish with the injection break frequency  $\nu_b$  in our model.

<sup>5</sup>  $x_{p_1} = 0.85$  and  $\phi_{p_1} = 0.5$  were adopted in the derivations according to Wijers & Galama (1999) and our obtained  $p_1 = 1.6$ .

To constrain the parameters, we require that (i) the R-band flux at 52 ks is  $F_{\nu_R}(52 \text{ ks}) = 55.9 \mu\text{Jy}^6$ , (ii)  $\nu_b(10 \text{ ks}) = 1.0 \times 10^{15} \text{ Hz}$ , and (iii)  $\nu_c$  should well above 10 keV at the last measurement of the X-ray afterglow, i.e.,  $\nu_c(2 \times 10^6 \text{ s}) > 10 \text{ keV}$ . After a simple calculation, we get

$$\epsilon_{B,-2} n_0^{2/3} = 1.95 \times 10^{-3} \epsilon_{e,-1}^{-4/3} E_{f,52}^{-5/3}, \quad (22)$$

$$\xi_4 = 1.5 \epsilon_{e,-1}^{-1/3} E_{f,52}^{0.24} n_0^{0.09}, \quad (23)$$

$$\epsilon_{e,-1} > 0.84 E_{f,52}^{-1}. \quad (24)$$

With only two equations, the model parameters ( $\epsilon_e$ ,  $\epsilon_B$ ,  $\xi$ ,  $E_f$  and  $n$ ) are strongly degenerate. Here we adopt a typical value of  $\epsilon_{e,-1} = 1$ , which has been supported by recent large sample afterglow modelings (e.g., Nava et al. 2014; Santana et al. 2014; Beniamini & van der Horst 2017).  $E_f$  is the final blast-wave energy after the energy injection, of which the mechanism was not specified above. Here we simply assume an equivalent prompt emission efficiency of  $\eta_\gamma = E_\gamma / (E_\gamma + E_f) = 10\%$  and leave the discussion on the energy injection mechanism in Section 5. With  $E_\gamma = 2.5 \times 10^{51} \text{ erg}$  and  $\eta_\gamma = 10\%$ , we obtain  $E_{f,52} = 2.25$  and Equation (24) is naturally satisfied. By substituting these values in Equation (22), we get  $\epsilon_{B,-2} n_0^{2/3} = 5.0 \times 10^{-4}$ . The values of  $\epsilon_B$  and  $n$  cannot be well constrained since both of them are highly uncertain parameters and vary over several orders of magnitude. By modeling the multi-band afterglows of 38 short GRBs, Fong et al. (2015) gave a median density of  $n \sim 10^{-3} - 10^{-2} \text{ cm}^{-3}$ , and found that 80%–95% of bursts have densities of  $n \lesssim 1 \text{ cm}^{-3}$ . For GRB 060614, if we take  $n_0 = 10^{-1}$  to  $10^{-3}$ , we get  $\epsilon_{B,-2} = 2.3 \times 10^{-3}$  to  $5 \times 10^{-2}$ . These values are well consistent with the recent results of Santana et al. (2014) and Barniol Duran (2014), who found the distribution of  $\epsilon_B$  has a range of  $\sim 10^{-8} - 10^{-3}$  with a median value of  $\sim \text{a few } \times 10^{-5}$ . In the following calculations, we adopt  $n_0 = 0.01$  and  $\epsilon_{B,-2} = 1.1 \times 10^{-2}$ . Finally, we substitute the above values in Equation (23) and get  $\xi_4 = 1.2$ . We note  $\xi$  is weakly dependent on other parameters and can be well constrained; it is around  $10^4$ , varying within a factor of two.

Since we interpret the achromatic break at  $t_{b,2}$  as a jet break, we can estimate the half-opening angle of the jet according to  $\theta_j \sim \gamma(t_j)^{-1}$  (Rhoads 1999; Sari et al.

<sup>6</sup> This value has been corrected for Galactic and host galaxy extinction with  $A_{V,G} = 0.07$  and  $A_{V,h} = 0.05$ , respectively, according to the results of M07.

1999). We thus have

$$\theta_j = 9.4^\circ E_{52}^{-1/8} n_0^{1/8} \left( \frac{t_{b,2,d}}{1+z} \right)^{3/8} = 5.1^\circ. \quad (25)$$

Using  $\gamma(t_j) \sim \theta_j^{-1} = 11.2$  and  $\gamma(t > t_j) \propto t^{-1/2}$  (Rhoads 1999), we have  $\gamma(2 \times 10^6 \text{ s}) \sim 2.7$ , which suggests a mildly relativistic jet even at the end of the X-ray observations. Therefore, our explanation of the entire afterglow of GRB 060614 in the relativistic regime is self-consistent.

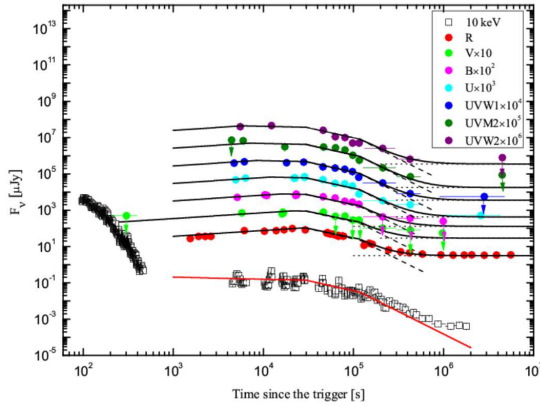


**Figure 1.** Theoretical LCs as compared with the multi-band afterglow observations of GRB 060614. The 10 keV unabsorbed X-ray data (empty squares) are downloaded from [http://www.swift.ac.uk/burst\\_analyser/00214805/](http://www.swift.ac.uk/burst_analyser/00214805/) (Evans et al. 2007, 2009). The *R*-band data (red filled circles) are taken from Della Valle et al. (2006) and Gal-Yam et al. (2006), while the optical/UV data in other bands are taken from M07. The optical/UV data have been corrected for Galactic and host galaxy extinction with  $A_{V,G} = 0.07$  and  $A_{V,h} = 0.05$ , respectively. For clarity, the shown flux densities in the *V*, *B*, *U*, *UVW1*, *UVM2* and *UVW2* bands have been rescaled by factors 10,  $10^2$ ,  $10^3$ ,  $10^4$ ,  $10^5$  and  $10^6$ , respectively. The red solid line is our model predicted X-ray LC. The modeled optical/UV LCs are shown as the sum (black solid lines) of two components: the afterglow (black dashed lines) and the host (black dotted lines). The magnitude values of the host in each band are taken from M07. To produce the theoretical LCs, the parameters of  $p_1 = 1.6$ ,  $p_2 = 2.68$ ,  $q = 0.41$ ,  $e = 0.27$ ,  $\epsilon_{e,-1} = 1$ ,  $\epsilon_{B,-2} = 1.1 \times 10^{-2}$ ,  $E_{f,52} = 2.25$ ,  $n_0 = 0.01$ ,  $\xi_4 = 1.2$ ,  $t_f = 29.7 \text{ ks}$  and  $t_j = 117.2 \text{ ks}$  are used.

Based on Equations (12), (13), (15), (18)–(21) and our obtained parameters, we can now compare our model with the multi-band afterglow LCs. As shown in Figure 1, the whole optical/UV and X-ray (except the last few data points) LCs can be well de-

scribed with our model<sup>7</sup>. Especially in the optical/UV band, our model successfully explained the initial frequency-dependent decay feature and the corresponding spectral evolution. Besides the two achromatic breaks  $t_{b,1}$  and  $t_{b,2}$ , there is an chromatic break  $t_\nu$  in the optical/UV LCs. It denotes the time that  $\nu_b$  crosses an observational frequency  $\nu$ . For  $\nu = R, V, B, U, UVW1, UVM2, UVW2$ , the corresponding breaks are  $t_\nu = 26.8, 21.1, 16.1, 12.0, 8.4, 7.0, 5.8 \text{ ks}$ . The optical/UV LCs show a plateau between  $t_\nu$  and  $t_{b,1}$  with the same slope as the X-ray plateau; before  $t_\nu$ , the LCs rise with a slope of  $(-0.32)$ . It should be noted that an exact calculation of afterglow radiation would give smooth spectral and temporal breaks (Granot & Sari 2002), so such a chromatic break in the optical/UV LCs may not be clearly seen, especially when the data are sparsely sampled. Instead, the passage of  $\nu_b$  through the optical/UV band may show an average effect in the LCs: slowly rising at low frequencies and flattening at higher energies, just like the afterglow of GRB 060614 (M07). We emphasize, however, that our simple analytic model perfectly described this feature and no need to employ complicated numerical calculations. For the X-ray afterglow, we note that the data points after  $\sim 10^6 \text{ s}$  obviously deviate from our modeling fit and suggest a late re-brightening or a flattening. M07 found that at the end the observations have small signal to noise ratios and approach the XRT sensitivity limit. We thus do not consider this inconsistency. There are also slight excesses between  $2 \times 10^5$  and  $10^6 \text{ s}$ , this is because in our modeling we used the central value of 2.48 for the post-jet-break slope. When the uncertainty of this parameter is considered, this problem would be alleviated.

We conclude this section by comparing the electron energy spectrum of GRB 060614 with that of GRB 091127. For GRB 091127, we have  $p_2 - p_1 = 1$ <sup>8</sup> and  $q = 0.64 \pm 0.08$  (Paper I). Correspondingly, GRB 060614 gives  $p_2 - p_1 = 1.08 \pm 0.20$  and  $q = 0.41 \pm 0.20$ . We emphasize that the values of  $q$  for both bursts are reliable, since the consistency checks have been performed with various afterglow observational constraints. Interestingly, both bursts show a similar value of  $\xi \sim 10^4$ , but at this stage we cannot exclude it is a coincidence. In summary, the two bursts suggest a possibly universal

<sup>7</sup> The initial steep decay of the X-ray LC before about 500 s is likely the prompt emission tail (M07) which is not a concern of our model.

<sup>8</sup> This is a natural result since Filgas et al. (2011) assumed  $\beta_X = \beta_{\text{opt}} + 0.5$  in their SED analysis. The true value of  $p_2 - p_1$  for this burst might not necessarily equal to 1, but it should be close to 1.

DPLH spectrum with  $p_2 - p_1 \sim 1$  and  $q \sim 0.5$ . However, it is likely premature to say so and more such events are needed to test this conjecture<sup>9</sup>. Finally, we emphasize that this DPLH spectrum predicts an injection break frequency evolving as  $\nu_b \propto t^{-3(1+q)/4} = t^{(-1.1)}$  (for  $e = 1$ ), which is substantially faster than  $\nu_c$  in a single PL hard electron spectrum model. Therefore, when this kind of spectral break along with flat spectra in the optical band are observed in the afterglow, it provides strong support to the above conjecture.

## 5. CONCLUSION AND DISCUSSION

Only a few GRB afterglows show very flat spectra in the optical band and require a hard ( $p < 2$ ) electron energy spectrum. Paper I showed that GRB 091127 gave tentative evidence for the exist of a DPLH spectrum with  $1 < p_1 < 2$ ,  $p_2 > 2$  and an injection break assumed as  $\gamma_b \propto \gamma^q$  in the relativistic regime. In this work, we show that of GRB 060614 provides further evidence for such a spectrum. This is supported by the flat spectra and the passage of a spectral break through the optical/UV band between  $\sim 10$  and  $\sim 30$  ks. In addition, the X-ray/UV LCs show an initial plateau lasting about 30 ks. We thus explain the multi-band afterglow with the DPLH model by taking into account an additional energy injection. Along with the results of GRB 091127, our work implies a possibly universal DPLH spectrum with  $p_2 - p_1 \sim 1$  and  $q \sim 0.5$ . However, more such afterglow observations are needed to test this conjecture.

Here we mention the work of Xu et al. (2009) who also modeled the multi-band afterglow of this burst. Different from our model, they used a standard ( $p > 2$ ) electron energy spectrum and interpreted the observed spectral break as  $\nu_m$ . This model was motivated by their SED analysis results at around 16 ks: the SED from the optical to X-ray bands was fitted by a broken PL which gave  $\beta_{\text{opt}} = -0.1 \pm 0.4$  (90% CL) and  $\beta_X = 0.9 \pm 0.1$  (90% CL). This spectrum is compatible with  $\nu_{\text{opt}} < \nu_m < \nu_X < \nu_c$  in the standard afterglow model. When an energy injection is assumed, this model can describe the afterglow LCs rather well (Xu et al. 2009). However, we should note that the value of  $\beta_{\text{opt}}$  cannot be well constrained in their fitting. Alternatively, the authors also fitted this SED by fixing  $\beta_X = \beta_{\text{opt}} + 0.5$  and gave  $\beta_{\text{opt}} \simeq 0.36$  and  $\beta_X \simeq 0.86$ . These values are remarkably consistent with those of M07. Both works

actually favor a positive  $\beta_{\text{opt}}$  which is not compatible with  $\nu_{\text{opt}} < \nu_m$ . Therefore, their model has difficulties in explaining the early flat spectra in the optical/UV band.

Our model assumes an additional energy injection process, we now discuss its possible origins. The energy injection can be provided by the central engine, e.g., a rapidly spinning, strongly magnetized neutron star (the so-called “millisecond magnetar”; e.g., Usov 1992; Thompson 1994; Dai & Lu 1998; Zhang & Mészáros 2001; Zhang et al. 2006; Rowlinson et al. 2013; Gompertz et al. 2014). However, the simplest dipole spin-down model predicts  $e = 0$  that is not consistent with our obtained  $e \sim 0.27$ . Modifications to the simplest model are needed for this burst. Alternatively, such an energy injection can be provided by the soft tail of the outflow by considering that the extended emission is several times more energetic than the initial hard pulse. To check the consistency with our obtained parameters in Section 4, we assume the energy injection takes place at  $t_i = 100$  s and take  $t_f = 29.7$  ks,  $E_f = 2.25 \times 10^{52}$  erg, then the initial kinetic energy of the outflow is  $E_i = E_f (t_i/t_f)^{(1-e)} \sim 3.5 \times 10^{50}$  erg. Since the isotropic energy of the initial pulse is also  $\sim 3.5 \times 10^{50}$  erg (Mangano et al. 2007), this corresponds a radiation efficiency of  $\sim 50\%$ , which is consistent the median value of short GRBs (Fong et al. 2015).

In our model, the steep post-jet-break decay of GRB 060614 is due to significant sideways expansion of the jet based on the theory of Rhoads (1999). However, our derived bulk Lorentz factor at the jet-break time is  $\sim 11$  that is highly relativistic. This is in conflict with the results given by numerical simulations and more sophisticated analytical treatments which suggest that the sideways expansion of a relativistic jet is not important until  $\gamma$  drops below  $\sim 2$  (Huang et al. 2000; Granot et al. 2001; Kumar & Granot 2003; Cannizzo et al. 2004; Zhang & MacFadyen 2009; de Colle et al. 2012; Granot & Piran 2012; van Eerten & MacFadyen 2012). There are also numerical works (e.g., Wygoda et al. 2011) supporting the simple analytic solutions of Rhoads (1999). Nevertheless, Granot & Piran (2012) found that exponential sideways expansion can only occur for jets with extremely narrow initial half-opening angle ( $\theta_0 \ll 0.05$ ) when  $\gamma \lesssim 1/\theta_j$  is satisfied. Considering that the realistic GRB jets may have much more complicated hydrodynamical evolutions than employed in the above analytic and numerical models, whether an early exponential sideways expansion phase exists for typical jet opening angles still remains uncertain. Observationally, a fraction of X-ray afterglows show a jet-

<sup>9</sup> The optical afterglow of GRB 060908 also shows a flat spectrum with  $\beta_{\text{opt}} \sim 0.3$  (Covino et al. 2010). As a test, we found its multi-band afterglow can be well explained with the DPLH model in a wind circumburst environment by assuming  $q \sim 0.5$ . Detailed calculations are now underway (Zhang et al. 2018, in preparation).



break-like feature at around 1 day with post-break slope of  $\sim p$  (e.g., Zhang et al. 2006; Willingale et al. 2007; Liang et al. 2008; Evans et al. 2009; Racusin et al. 2009; Panaitescu & Vestrand 2012); some recent systematic studies of multi-band afterglows have also shown that a small fraction of GRBs have such jet-break features, simultaneously in X-rays and in the optical band (e.g., Fong et al. 2015; Li et al. 2015; Wang et al. 2015). Therefore, at least for some GRBs, sideways expansion should be significant when  $\gamma \lesssim 1/\theta_j$  is satisfied, even though the jet is still in the relativistic regime.

Finally, we give a discussion on the DPLH spectrum and the value of  $q$ . In the original work of Bhattacharya & Resmi (2004), the authors assumed the injection break to be the minimum electron Lorentz factor that can be accelerated by relativistic shocks, i.e.,  $\gamma_b \equiv \gamma_{\text{acc}} = (m_p/m_e)\gamma$ ; between  $\gamma_m$  and  $\gamma_b$ , some other acceleration mechanisms take place and produce a hard electron spectrum. This means  $q = 1$  in their model. However, our work suggests  $q \sim 0.5$  that disfavors this scenario. Moreover, the value of  $\xi$  we derived is much larger than  $m_p/m_e$ . (Resmi & Bhattacharya 2008) extended this function by assuming  $\gamma_b \propto (\beta\gamma)^q$  and attempted to find evidence by modeling the afterglows of three pre-*Swift* GRBs. Although their model can explain the afterglow LCs, the evidence for a DPLH spectrum is far from robust. First, no bursts in their sample show very flat spectra in the optical band. Their spectral indices are in the range of 0.6–0.9 that is typical for optical afterglows (e.g., Li et al. 2012). Second, no spectral evolution was seen in their sample. That is, the injection

break frequency  $\nu_b$  was actually not observed directly. Finally, for these bursts, the DPLH model is not the sole explanation. The LCs can also be reproduced by a model assuming continuous energy injection (e.g., Björnsson et al. 2002). Besides, their derived model parameters are much different from ours (see Paper I for a detailed discussion). Especially on the value of  $q$ , they gave  $q \gtrsim 1$  for all bursts, while ours is substantially smaller. Since our works have provided the most robust evidence for a DPLH spectrum so far,  $q \sim 0.5$  should be preferred.

The origin of the hard electron energy distribution is not clear. Our results may offer guidance in the right direction. Meanwhile, more observations of GRB afterglows with a hard electron spectrum and further developments in the area of simulations of the *Fermi* acceleration process in relativistic shocks will help us understand the origin of the observed spectra of GRBs and their afterglows.

This work made use of data supplied by the UK Swift Science Data Centre at the University of Leicester. This study was supported by the Strategic Priority Research Program of the Chinese Academy of Sciences (Grant No. XDB23040400). SLX was also supported by the Hundred Talents Program of the Chinese Academy of Sciences (Grant No. Y629113). LMS acknowledges support from the National Program on Key Research and Development Project (Grant No. 2016YFA0400801) and the National Basic Research Program of China (Grant No. 2014CB845802).

## REFERENCES

- Achterberg, A., Gallant, Y. A., Kirk, J. G., & Guthmann, A. W. 2001, *MNRAS*, 328, 393
- Baring, M. G. 2004, *NuPhS*, 136, 198
- Barniol Duran, R. 2014, *MNRAS*, 442, 3147
- Barthelmy, S. D., Barbier, L. M., Cummings, J. R., et al. 2005, *SSRv*, 120, 143
- Barthelmy, S., Barbier, L., Cummings, J., et al. 2006, *GCN*, 5256, 1
- Bednarz, J., & Ostrowski, M. 1998, *PhRvL*, 80, 3911
- Beniamini, P., & van der Horst, A. J. 2017, *MNRAS*, 472, 3161
- Bhattacharya, D. 2001, *BASI*, 29, 107
- Bhattacharya, D., Resmi, L. 2004, in *ASP Conf. Ser.* 312, *Evolution of an Afterglow with a Hard Electron Spectrum*, ed. M. Feroci et al. (San Francisco, CA: ASP), 411
- Björnsson G., Hjorth J., Pedersen K., & Fynbo J. U. 2002, *ApJL*, 579, L59
- Blandford, R. D., & McKee, C. F. 1976, *PhFl*, 19, 1130
- Burrows, D. N., Hill, J. E., Nousek, J. A., et al. 2005, *SSRv*, 120, 165
- Cannizzo, J. K., Gehrel, N., & Vishniac, E. T. 2004, *ApJ*, 601, 380
- Chevalier, R. A., & Li, Z.-Y. 2000, *ApJ*, 536, 195
- Covino S., Campana S., Conciatore M. L., et al. 2010, *A&A*, 521, A53
- Curran, P. A., Evans, P. A., de Pasquale, M., Page, M. J., & van der Horst, A. J. 2010, *ApJL*, 716, L135
- Curran, P. A., Starling, R. L. C., van der Horst, A. J., & Wijers, R. A. M. J. 2009, *MNRAS*, 395, 580
- Dai, Z. G., & Cheng, K. S. 2001, *ApJL*, 558, L109
- Dai, Z. G., & Lu, T. 1998, *A&A*, 333, L87
- de Colle, F., Ramirez-Ruiz, E., Granot, J., & Lopez-Camara, D. 2012, *ApJ*, 751, 57
- Della Valle, M., Chincarini, G., Panagia, N., et al. 2006, *Natur*, 444, 1050

- Evans, P. A., Beardmore, A. P., Page, K. L., et al. 2007, *A&A*, 469, 379
- Evans, P. A., Beardmore, A. P., Page, K. L., et al. 2009, *MNRAS*, 397, 1177
- Fermi, E. 1954, *ApJ*, 119, 1
- Filgas, R., Greiner, J., Schady, P., et al. 2011, *A&A*, 537, A57
- Fong, W., Berger, E., Margutti, R., & Zauderer, B. A. 2015, *ApJ*, 815, 102
- French, J., Melady, D., Hanlon, L., Jelínek, M., & Kubánek, P. 2006, *GCN*, 5257, 1
- Fugazza, D., Malesani, D., Romano, P., et al. 2006, *GCN*, 5276, 1
- Fynbo, J. P. U., Watson, D., Thöne, C. C., et al. 2006, *Natur*, 444, 1047
- Gal-Yam, A., Fox, D. B., Price, P. A., et al. 2006, *Natur*, 444, 1053
- Gao, H., Lei, W. H., Zou, Y. C., Wu, X. F., & Zhang, B. 2013, *NewAR*, 57, 141
- Gehrels, N., Norris, J. P., Barthelmy, S. D., et al. 2006, *Natur*, 444, 1044
- Golenetskii, S., Aptekar, R., Mazets, E. 2006, *GCN*, 5264, 1
- Gompertz, B. P., O’Brien, P. T., & Wynn, G. A. 2014, *MNRAS*, 438, 240
- Granot, J., Miller, M., Piran, T., Suen, W. M., & Hughes, P. A. 2001, in *Gamma-ray Bursts in the Afterglow Era, Light Curves from an Expanding Relativistic Jet*, ed. E. Costa, F. Frontera & J. Hjorth, 312
- Granot, J., & Piran, T. 2012, *MNRAS*, 421, 570
- Granot, J., & Sari, R. 2002, *ApJ*, 568, 820
- Holland, S. T. 2006, *GCN*, 5255, 1
- Huang, Y. F., Gou, L. J., Dai, Z. G., & Lu, T. 2000, *ApJ*, 543, 90
- Jarosik, N., Bennet, C. L., Dunkley, J., et al. 2011, *ApJS*, 192, 14
- Jin, Z. P., Li, X., Cano, Z., et al. 2015, *ApJL*, 811, L22
- Kirk, J. G., Guthmann, A. W., Gallant, Y. A., & Achterberg, A. 2000, *ApJ*, 542, 235
- Kumar, P., & Granot, J. 2003, *ApJ*, 591, 1075
- Lemoine, M., & Pelletier, G. 2003, *ApJL*, 589, L73
- Li, L., Liang, E. W., Tang, Q. W., et al. 2012, *ApJ*, 758, 27
- Li, L., Wu, X. F., Huang, Y. F. et al. 2015, *ApJ*, 805, 13
- Liang, E. W., Racusin, J. L., Zhang, B., Zhang, B. B., & Burrows, D. N. 2008, *ApJ*, 675, 528
- Mangano, V., Holland, S. T., Malesani, D., et al. 2007, *A&A*, 470, 105 (M07)
- Melandri, A., Bernardini, M. G., D’Avanzo, P., et al. 2015, *A&A*, 581, A86
- Mészáros, P., & Rees, M. J. 1993, *ApJ*, 405, 278
- Mészáros, P., & Rees, M. J. 1997, *ApJ*, 476, 232
- Mészáros, P., & Rees, M. J. 1999, *MNRAS*, 306, L39
- Nava, L., Vianello, G., Omodei, N., et al. 2014, *MNRAS*, 443, 3578
- Nousek, J. A., Kouveliotou, C., Grupe, D., et al. 2006, *ApJ*, 642, 389
- Panaitescu, A., & Kumar, P. 2001, *ApJ*, 554, 667
- Panaitescu, A., & Kumar, P. 2002, *ApJ*, 571, 779
- Panaitescu, A., & Vestrand, W. T. 2012, *MNRAS*, 425, 1669
- Parsons, A. M., Cummings, J. K., Gehrels, N. 2006, *GCN*, 5252, 1
- Price, P. A., Berger, E., & Fox, D. B. 2006, *GCN*, 5275, 1
- Racusin, J. L., Liang, E. W., Burrows, D. N., et al. 2009, *ApJ*, 698, 43
- Rees, M. J., & Mészáros, P. 1992, *MNRAS*, 258, 41
- Rees, M. J., & Mészáros, P. 1998, *ApJL*, 496, L1
- Resmi, L., & Bhattacharya, D. 2008, *MNRAS*, 388, 144
- Rhoads, J. E. 1999, *ApJ*, 525, 737
- Roming, P. W. A., Kennedy, T. E., Mason, K. O., et al. 2005, *SSRv*, 120, 95
- Rowlinson, A., O’Brien, P. T., Metzger, B. D., Tanvir, N. R., & Levan, A. J. 2013, *MNRAS*, 430, 1061
- Santana, R., Barniol Duran, R., & Kumar, P. 2014, *ApJ*, 785, 29
- Sari, R., & Mészáros, P. 2000, *ApJL*, 535, L33
- Sari, R., Piran, T., & Halpern, J. P. 1999, *ApJL*, 519, L17
- Sari, R., Piran, T., & Narayan, R. 1998, *ApJL*, 497, L17
- Shen, R., Kumar, P., & Robinson, E. L. 2006, *MNRAS*, 371, 1441
- Spitkovsky, A. 2008, *ApJL*, 682, L5
- Starling, R. L. C., Van der Horst, A. J., Rol, E., et al. 2008, *ApJ*, 672, 433
- Thompson, C. 1994, *MNRAS*, 270, 480
- Troja, E., Sakamoto, T., Guidorzi, C., et al. 2012, *ApJ*, 761, 50
- Usov, V. V. 1992, *Natur*, 357, 472
- van Eerten, H. J., & MacFadyen, A. I. 2012, *ApJ*, 751, 155
- Wang, X. G., Zhang, B., Liang, E. W., et al. 2015, *ApJ*, 219, 9
- Wang, Y., Fan, Y. Z., Wei, D. M., & Stefano, C. 2012, *ChA&A*, 36, 148
- Wijers, R. A. M. J., & Galama, T. J. 1999, *ApJ*, 523, 177
- Willingale, R., O’Brien, P. T., Osborne, J. P., et al. 2007, *ApJ*, 662, 1093
- Wygoda, N., Waxman, E., & Frail, D. 2011, *ApJL*, 738, L23
- Xu, D., Starling, R. L. C., Fynbo, J. P. U., et al. 2009, *ApJ*, 696, 971
- Yang, B., Jin, Z. P., Li, X., et al. 2015, *NatCo*, 6, 7323
- Zaninoni, E., Bernardini, M. G., Margutti, R., Oates, S., & Chincarini, G. 2013, *A&A*, 557, A12

Zhang, B., Fan, Y. Z., Dyks, J., et al. 2006, ApJ, 642, 354

Zhang, B., & Mészáros, P. 2001, ApJL, 552, L35

Zhang, B., Zhang, B. B., Liang, E. W., et al. 2007, ApJ, 655, L25

Zhang, Q., Huang, Y. F., & Zong, H. S. 2015, ApJ, 811, 83, (Paper I)

Zhang, W., & MacFadyen, A. 2009, ApJ, 698, 1261